Front. Optoelectron. 2012, 5(2): 187–194
DOI 10.1007/s12200-012-0231-8

RESEARCH ARTICLE

Simplified adaptively modulated optical OFDM modems using subcarrier modulation with added input/output reconfigurability

Xing ZHENG, Jinlong WEI, Roger Philip GIDDINGS, Jianming TANG (✉)

School of Electronic Engineering, Bangor University, Bangor, LL57 1UT, UK

Abstract Three novel designs of adaptively modulated optical orthogonal frequency division multiplexing modems using subcarrier modulation (AMOOFDM-SCM) are proposed, for the first time, each of which requires a single inverse fast Fourier transform/fast Fourier transform (IFFT/FFT) operation. These designs not only significantly simplify the AMOOFDM-SCM modem configurations, but also offer extra unique network features such as input/output reconfigurability. Investigations show that these three modems are capable of supporting more than 60 Gb/s AMOOFDM-SCM signal transmission over 20, 40 and 60 km single mode fibre (SMF)-based intensity modulation and direct detection (IMDD) transmission links without optical amplification and chromatic dispersion compensation.

Keywords orthogonal frequency division multiplexing (OFDM), subcarrier modulation (SCM), single mode fibre (SMF)

1 Introduction

Owing to its strong intrinsic tolerance to fibre chromatic dispersion and polarization mode dispersion, efficient use of spectral characteristics of transmission links, relatively high signal transmission capacity, significant system flexibility and potentially low system cost, optical orthogonal frequency division multiplexing (OOFDM) has been considered as one of the most promising candidates for high signal capacity transmission in next-generation optical networks of various architectures [1–3]. In particular, adaptively modulated OOFDM (AMOOFDM) has demonstrated great potential for providing a high-speed and cost-effective solution for practical implementation in cost-sensitive, intensity modulation and direct detection (IMDD) optical networks such as multi-mode fibre (MMF)-based local area networks [4] and single mode fibre (SMF)-based access and metropolitan area networks [1].

AMOOFDM has a unique feature that the signal modulation format taken on each subcarrier can be varied according to the frequency response of a given transmission system. Generally speaking, a high (low) signal modulation format is used on a subcarrier experiencing a high (low) signal-to-noise ratio (SNR). Any subcarriers suffering very low SNRs may be dropped completely if there are still a large number of errors occurred even when the lowest signal modulation format is used. As a direct result, AMOOFDM effectively utilizes the IMDD transmission system frequency response, the major portion of which is, however, still unused.

To make a full use of the frequency response of a transmission system, subcarrier modulation (SCM) [5] can be employed, in which a baseband signal is modulated onto a radio frequency (RF) carrier directly driving an electrical-to-optical intensity modulator. Unfortunately, the transmission performance of the SCM technique is relatively low, as SCM does not have the capability of manipulating the signal modulation format within each SCM subcarrier. By introducing SCM into AMOOFDM, an AMOOFDM modem using SCM (AMOOFDM-SCM) has been proposed [6], which consists of two parallel conventional AMOOFDM modems that produce two real-valued double sideband (DSB) SCM subcarriers with one operating at the baseband and the other being modulated onto an intermediate RF carrier. For MMF-based IMDD transmission systems, when compared with AMOOFDM, AMOOFDM-SCM not only doubles the signal transmission capacity versus reach performance, but also

Received November 28, 2011; accepted December 8, 2011

E-mail: j.tang@bangor.ac.uk

considerably relaxes the minimum requirement on key components involved in the AMOOFDM-SCM modems [6].

For SMF-based IMDD transmission systems, the cross-talk effect induced by beating among different subcarriers of various types upon direct detection in the receiver is a dominant factor limiting the maximum achievable AMOOFDM-SCM performance. To mitigate such an effect, three AMOOFDM-SCM schemes, known as AMOOFDM-SCM scheme I, II and III, have been proposed for different application scenarios [7]. AMOOFDM-SCM scheme I uses two real-valued DSB SCM subcarriers, with one operating at the baseband and the other being modulated onto an intermediate RF carrier. AMOOFDM-SCM scheme II is formed by inserting, between the optical carrier and the baseband SCM subcarrier of scheme I, a spectral gap having a width of twice of the SCM subcarrier bandwidth. In AMOOFDM-SCM scheme III, single sideband (SSB) modulation in the electrical domain is applied to the two SCM subcarriers of AMOOFDM-SCM scheme II. It has been shown that, AMOOFDM-SCM scheme I, II and III are capable of supporting more than 60 Gb/s signal transmission over 60 km SMFs in IMDD systems without optical amplification and chromatic dispersion compensation [7].

However, in each of the aforementioned AMOOFDM-SCM schemes, two inverse fast Fourier transform (IFFT/FFT) operations are required to produce two real-valued SCM subcarriers. As the IFFT and FFT are the most computationally intense functions and require significant amount of logic resources in each AMOOFDM modem [8], this design may increase the system complexity and cost.

To address the above-mentioned challenge, in this paper, three significantly simplified AMOOFDM-SCM modem configurations, referred to as reconfigurable scheme (RS) I, II and III, are proposed, for the first time, each of which requires a single IFFT/FFT operation only. The general structures of the three proposed RS modems are similar to those corresponding to these AMOOFDM-SCM schemes [7]. The considerable differences between these two sets of modems are the signal processing approaches used in distributing the encoded incoming data prior to the IFFT operation in the transmitter and those adopted in recovering the received data after the FFT operation in the receiver, as discussed in Section 2.

Investigations show that the RS modem configurations support transmission performances identical to those presented in Ref. [7] without compromising system flexibility and performance robustness to variations in transmission link characteristics. More importantly, the simplified RS modems also offer input/output reconfigurability: in the transmitter, the input data can be either from two independent data sources, or from a single data source, which is then split into two sets of data. For simplicity, here these two sets of data are denoted as $\{A\}$ and $\{B\}$. As shown in Section 2, an appropriate arrangement of these two sets of data at the input of the IFFT operation enables that the in-phase (I) and quadrature (Q) components at the output of the IFFT operation convey information only from $\{A\}$ and $\{B\}$, respectively. Therefore, $\{A\}$ and $\{B\}$ can be recovered independently by two individual end-users in the receiver. Alternatively, these two sets of data can also be recovered simultaneously by a single end-user using a similar receiver. It is also worth mentioning that coherent OOFDM [9] or OOFDM based on complex RF up-conversion [3] is not capable of offering the above-mentioned input/output reconfigurability, as the resulting I and Q components in the transmitter are not separable.

Apart from the features mentioned above, when use is made of the proposed RS modems in access networks such as wavelength division multiplexed passive optical networks (WDM-PONs), as discussed in Section 3, the RS modems also reveal the following salient advantages: 1) supporting the doubled number of end-users without increasing the number of wavelengths; 2) significantly reducing system complexity and cost when compared to conventional AMOOFDM-SCM schemes, and 3) providing a number of extra network functionalities including for example dynamic bandwidth allocation, broadcasting functionality and network monitoring. It should be noted that, the proposed RS modems inherit all the advantages of conventional AMOOFDM-SCM including, for example, significant relaxation of the minimum requirements on key component parameters, excellent performance robustness to variations in transmission link characteristics and efficient utilization of link frequency response characteristics.

The paper is organized as follows. In Section 2, the simplified RS modems are described with special attention being given to the signal processing approaches for distributing (recovering) data before the IFFT (after the FFT). In Section 3, the advantages of utilizing the RS modems in WDM-PON systems are discussed in detail. In Section 4, the transmission performance of the proposed RS modems are presented and discussed. Finally, the paper is summarized in Section 5.

2 Reconfigurable modem designs

Since RS III is of the highest complexity among the three RS modems proposed, in Fig. 1, the schematic transceiver diagram of RS III is illustrated, whose operating principles are described below. The corresponding information for RS I and II is, however, not presented in detail here, as it can be understood easily using RS III and AMOOFDM-SCM scheme I and II. The signal spectra of the three proposed RS modems are illustrated in Fig. 2. A single-channel IMDD SMF transmission link operating at 1550 nm is considered, in which optical amplification and chromatic dispersion compensation are excluded.

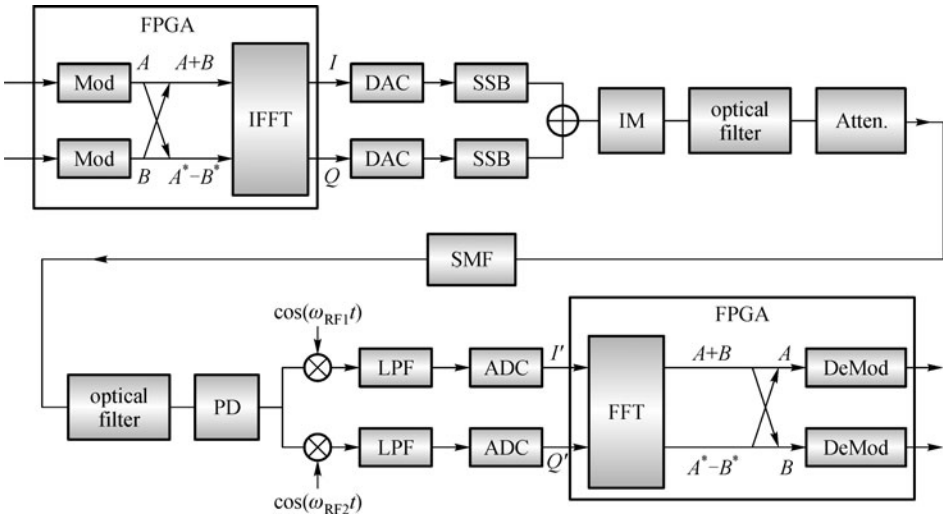

Fig. 1 Schematic illustration of RS III modem configuration and corresponding transmission link structure. Mod: modulation; IM: intensity modulator; Atten.: attenuator; PD: photodetector; DeMod: demodulation; FPGA: field programmable gate array; DAC/ADC: digital-to-analogue converter/analogue-to-digital converter; LPF: low-pass filter

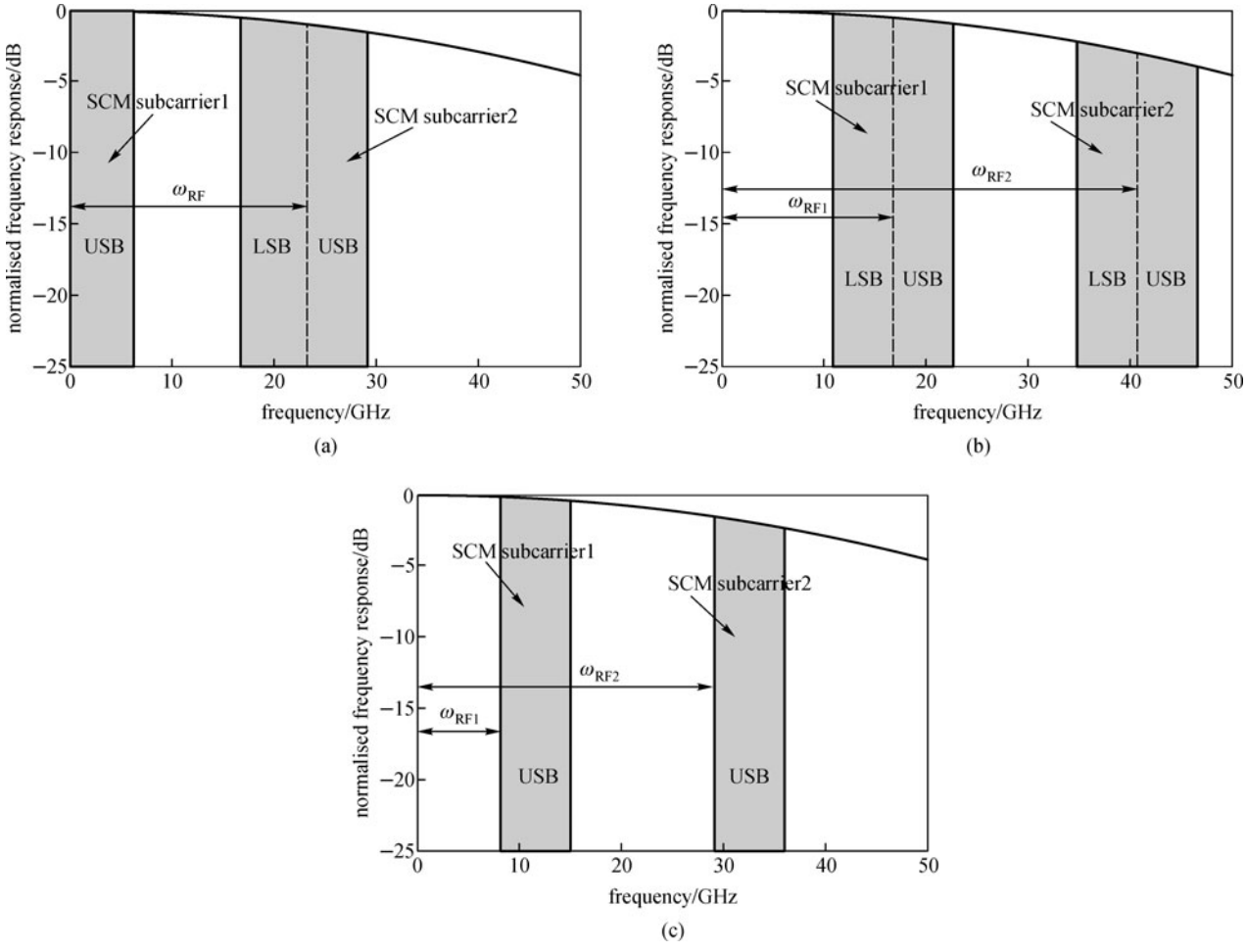

Fig. 2 Signal spectra of proposed RS modems. USB: upper sideband spectrum of SCM subcarrier; LSB: lower sideband spectrum of SCM subcarrier. (a) RS I; (b) RS II; (c) RS III

In all the AMOOFDM-SCM transmitters reported previously [6,7], AMOOFDM subcarriers, which consist of a total number of $2N$ parallel data including both the encoded original data and their conjugate counterparts, are arranged at the input of the IFFT to satisfy the Hermitian symmetry. For each individual modem, such an input data arrangement leads to the generation of a real-valued SCM subcarrier and zero from the real and imaginary IFFT output ports, respectively. Given the complex property of the IFFT, only half of the IFFT output ports are employed for transmission.

In the proposed RS I, II and III transmitters, AMOOFDM subcarriers are a sum of two individual sets of data, $\{A\}$ and $\{B\}$, each of which contains $2N$ parallel encoded data. When the n-th elements of $\{A\}$ and $\{B\}$ satisfy $A_{2N-n} = A_n^*$ and $B_{2N-n} = -B_n^*$ for n = 1,2, …,$2N-1$, as well as $\mathrm{Im}\{A_0\} = \mathrm{Im}\{A_N\} = \mathrm{Im}\{B_0\} = \mathrm{Im}\{B_N\} = 0$, as illustrated in Fig. 3, after applying the IFFT operation to the sum of $\{A\}$ and $\{B\}$, a k-th output symbol can be written as

$$S_k^{A+B}(t) = \sum_{n=0}^{2N-1} A_n e^{j2\pi n\Delta f t} + \sum_{n=0}^{2N-1} B_n e^{j2\pi n\Delta f t} = I_{k\_A}(t) + jQ_{k\_B}(t), \quad (1)$$

where Δf is the frequency spacing between two adjacent AMOOFDM subcarriers. Equation (1) indicates that the input data distribution adopted here enables full use of both components, $I_{k\_A}(t)$ and $Q_{k\_B}(t)$. More importantly, $I_{k\_A}(t)$ conveys information only from $\{A\}$ and $Q_{k\_B}(t)$ conveys information only from $\{B\}$. Such a feature enables the independent transmission of two sets of data with a single IFFT operation being involved. $I_{k\_A}(t)$ and $Q_{k\_B}(t)$ are then used to generate two SCM subcarriers, which are transformed into two real-valued DSB baseband analogue SCM subcarriers, $A_{\mathrm{DSB1}}(t)$ and $A_{\mathrm{DSB2}}(t)$, following a number of operations including cyclic prefix insertion, parallel-to-serial conversion and digital-to-analogue conversion.

To reduce the subcarrier × subcarrier beating-induced cross-talk effect, in RS III, a phase-shift method based on the Hilbert transform [10] is applied to $A_{\mathrm{DSB1}}(t)$ and $A_{\mathrm{DSB2}}(t)$ to generate two real-valued SSB SCM subcarriers, $S_{\mathrm{SSB1}}(t)$ and $S_{\mathrm{SSB2}}(t)$, which can be expressed as

$$S_{\mathrm{SSB}m}(t) = A_{\mathrm{DSB}m}(t)\cos(\omega_{\mathrm{RF}m}t) - H\{A_{\mathrm{DSB}m}(t)\}\sin(\omega_{\mathrm{RF}m}t), \quad m = 1,2, \quad (2)$$

where $H\{A_{\mathrm{DSB}m}(t)\}$ is the Hilbert transform of $A_{\mathrm{DSB}m}(t)$. $\omega_{\mathrm{RF}m}$ is the intermediate RF frequency corresponding to the m-th SCM subcarrier within an AMOOFDM-SCM signal.

An intensity modulator is driven directly by

$$S_e(t) = S_{\mathrm{SSB1}}(t) + S_{\mathrm{SSB2}}(t) + I_{\mathrm{DC}}, \quad (3)$$

where I_{DC} is the added DC component to ensure that $S_e(t)$ is always positive. $S_{\mathrm{SSB1}}(t)$ and $S_{\mathrm{SSB2}}(t)$ are linearly scaled to have identical electrical powers. For simplicity, an ideal intensity modulator is assumed, which produces optical output signals having waveforms governed by $S_o(t) = \sqrt{S_e(t)}$ [7]. As a semiconductor optical amplifier (SOA) operating at a strongly saturated optical gain region has an effective bandwidth comparable to the entire AMOOFDM-SCM signal bandwidth [11], the SOA can, therefore, be utilized to perform such intensity modulation. Compared to Mach-Zehnder intensity modulators, the use of SOA intensity modulators is very cost-effective and can avoid conducting compensation for I/Q imbalance and bias deviation, thus resulting in the simplified modem design and cost reduction [12]. In addition, the SOA intensity modulators can also support colourless transmitters [13]. An ideal optical filter is also introduced to produce optical SSB signals for all transmission cases considered in this paper.

At the output facet of the SMF link, the transmitted optical signal is converted into the electrical domain by a square-law photodetector. After independently performing RF down-conversion using different RF frequencies, and undertaking, in a reverse procedure compared to the transmitter, a sequence of essential signal processing operations required prior to the FFT, two digital baseband SCM subcarriers are obtained. When both of these baseband SCM subcarriers are used as the inputs to the real and imaginary input ports of the FFT operation, both $\{A\}$ and $\{B\}$ can be recovered simultaneously by making use of the formulas

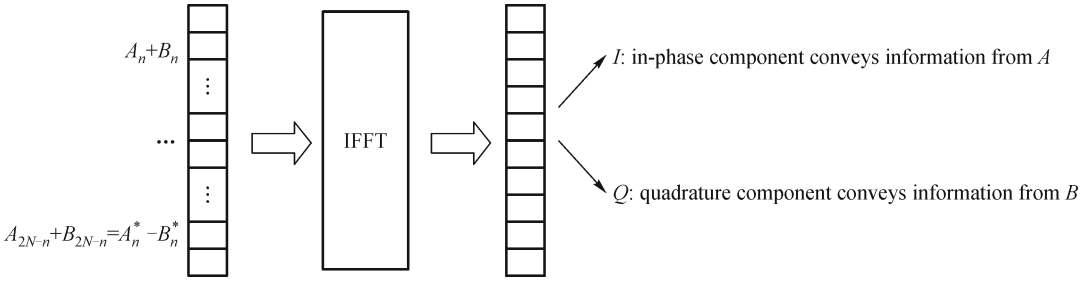

Fig. 3 Illustration of generation of pure real-valued symbols and pure imaginary-valued symbols

$$A_n = \frac{1}{2}\{[\mathrm{Re}(S'_n) + \mathrm{Re}(S'_{2N-n})] + \mathrm{j}[\mathrm{Im}(S'_n) - \mathrm{Im}(S'_{2N-n})]\}, \quad (4)$$

$$B_n = \frac{1}{2}\{[\mathrm{Re}(S'_n) - \mathrm{Re}(S'_{2N-n})] + \mathrm{j}[\mathrm{Im}(S'_n) + \mathrm{Im}(S'_{2N-n})]\}, \quad (5)$$

where S'_n is the n-th AMOOFDM subcarrier at the FFT output. On the other hand, when use is made of a single baseband SCM subcarrier, only $\{A\}$ or $\{B\}$ can be recovered directly without requiring Eqs. (4) and (5). It should be noted, in particular, that the aforementioned data recovering processes are independent upon each other and can take place simultaneously, when a dedicated FFT operation is provided for the selected SCM subcarrier(s). Clearly, the aforementioned input/output reconfigurability also holds for RS I and II.

3 Adanvantages of RS modems for acess networks

Compared to conventional AMOOFDM-SCM schemes, the RS schemes not only simplify the modem configurations due to the employment of a single IFFT/FFT in the transmitter/receiver, but also offer input/output reconfigurability. These features can bring a number of salient advantages when use is made of the RS modems in WDM-PONs. The advantages are listed as follows:

Dynamic bandwidth allocation capability: In pure WDM-PONs, one optical channel having a fixed bandwidth is assigned to one dedicated end-user only. Without requiring any modifications to the fibre infrastructure and by using a single optical channel only, the use of the RS modems allows two end-users to share dynamically a total bandwidth of twice of that corresponding to a single end-user. Clearly, this capability can offer bandwidth saving if a single end-user does not require the service in a specific time slot. In addition, the dynamic bandwidth allocation capability is also able to realize service classification [14] by carrying high priority services via one of the data sets $\{A\}$ or $\{B\}$, and the rest services via the other data set.

Doubled number of end-users: In comparison with the number of end-users supported by a pure WDM-PON having a specific number of optical wavelengths, the employment of the RS modems in such a network is able to double the number of end-users served without compromising the bandwidth offered to each end-user.

Broadcasting functionality: Instead of transmitting end-user data, one of the data sets can be utilised to carry a broadcasting signal, which is distributed to each end-user along with its own traffic carried by the other data set. Therefore, network services such as video overlay [15] can be simply realized by this broadcasting functionality without changing network infrastructure and the attached transceivers.

Network monitoring functionality: As discussed in Section 2, $\{A\}$, $\{B\}$ and $\{A\}+\{B\}$ can be recovered simultaneously and independently. This indicates that use can be made of the RS modems to perform network functionalities such as network monitoring and resilience. Generally speaking, the RS modems can have a structure of three independent receivers. Two receivers for two end-users to receive data $\{A\}$ and $\{B\}$ respectively, while the third receiver to collect the combination of data traffic $\{A\}$ and $\{B\}$ in order to check the network resilience simultaneously.

Cost reduction: When compared to conventional AMOOFDM-SCM schemes, the use of the RS modems in WDM-PONs brings significant cost savings, due to their features including, for example, simplified modem configurations and doubled number of end-users served.

In addition, it can be easily estimated that, compared to conventional AMOOFDM-SCM, the RS modems can not only bring potentially reductions in power consumptions, but also significantly simplify synchronization processes as the RS modems can omit precise time synchronization of two parallel AMOOFDM modems required in an conventional AMOOFDM-SCM modem.

4 Transmission performance

In simulating the transmission performances of RS I, II and III, 64 AMOOFDM subcarriers are considered, of which 31 having identical powers carry real data and one has no power. The modulation formats taken on each AMOOFDM subcarrier vary from differential binary phase shift keying (DBPSK), differential quadrature phase shift keying (DQPSK), and 16 to 256 quadrature amplitude modulation (QAM), depending on the frequency response of a specific transmission link. The cyclic prefix (CP) parameter defined in Ref. [16] is chosen to be 25%. It should be noted that the CP length required by the transmission links considered in this paper can be reduced, leading to an improved transmission performance [17]. However, to examine the validity of the proposed RS modems, fair comparisons are necessary between the results presented here and those obtained in Ref. [7], a CP value of 25% is, therefore, considered in this paper. The DAC/ADC operates at 12.5 GS/s and 7-bit quantization. Based on these parameters, each SCM subcarrier has a bandwidth of 6.25 GHz. To reduce the peak-to-average power ratio, signal clipping is applied to each of the SCM subcarriers, and the clipping level defined in Ref. [16] is taken to be 13 dB, which is an optimum value identified in Ref. [18]. Optical powers coupled into the SMF links are fixed at 6.3 dBm. All other parameters that are not explicitly mentioned above can be found in Ref. [7].

In addition, a comprehensive theoretical SMF model and a photodetector model are adopted, both of which are employed successfully in Refs. [1,7].

To demonstrate the maximum achievable signal transmission performances of the proposed RS modems, the signal line rate is defined as

$$R_s = \sum_{m=1}^{2} \frac{\sum_{k=1}^{31} M_{mk}}{(2N + N_{cp})T_s}, \quad (6)$$

where m is the index of the SCM subcarriers. M_{mk} is the number of binary bits carried by the k-th AMOOFDM subcarrier in the m-th SCM subcarrier. N_{cp} is the number of samples occupied by the cyclic prefix. T_s is the ADC sampling period. A R_s corresponding to a total channel bit error rate (BER) of less than 1.0×10^{-3} is considered to be valid. The BER is obtained by using direct error counting within 1400 OFDM symbols, which are oversampled to give a total number of sample points of 1024976 per data sequence.

When use is made of the RS modems, the maximum achievable transmission capacity for each optical channel depends on the intermediate RF frequency of the SCM subcarrier in each RS modem. For a given transmission link, an appropriate frequency adjustment is essential to position the SCM subcarrier in a desired link frequency response region, where the SCM subcarrier suffers a relatively low transmission loss and simultaneously the reduced cross-talk effect. To identify the optimum SCM subcarrier frequencies of the three RS modems, the transmission capacities versus RF frequency for 40 km SMF transmission links are shown in Fig. 4, where the corresponding behaviours are also given for conventional AMOOFDM-SCM modems.

Figure 4(a) shows ω_{RF1} dependent transmission performances of RS II and III for fixed ω_{RF2} values of 45 GHz (RS II) and 38 GHz (RS III). Upon direct detection in the receiver, beatings between different AMOOFDM subcarriers of the same SCM subcarrier produce an unwanted spectral distortion region occurring in the vicinity of the optical carrier. Such a spectral distortion region has a bandwidth of twice of the SCM subcarrier bandwidth [7]. The use of ω_{RF1} is to separate such an unwanted spectral region from the useful SCM subcarrier spectrum. Taking into account Fig. 2, discussions in Section 2 and the simulation parameters listed above, it is very easy to understand that the optimum ω_{RF1} values for RS II and III are approximately 19 and 12 GHz, respectively, as seen in Fig. 4(a). A ω_{RF1} value lower than the optimum value increases the overlap between the spectral distortion region and the first SCM subcarrier. On the other hand, a ω_{RF1} value higher than the optimum one enhances not only the cross-talk effect between the two SCM subcarriers, but also the transmission loss experienced by the first SCM subcarrier. The origin of the frequency dependent transmission loss effect is due to the fact that an IMDD transmission link has a Gaussian-shaped frequency response with its peak occurring at the optical carrier, and the frequency response becomes narrow for a long transmission distance [1, 8,17,18].

Based on the identified optimum ω_{RF1} values for different RS modems, ω_{RF2} dependent transmission performances of RS I, II and III are shown in Fig. 4(b), from which the optimum ω_{RF2} values of approximately 20, 45 and 38 GHz are identified for RS I, II and III, respectively. The beating between different SCM subcarriers causes the generation of unwanted products occurring at a spectral region between the two SCM subcarriers. A decrease in ω_{RF2} increases the cross-talk effect. On the other hand, as explained above, a large ω_{RF2} value results in a high transmission loss. The co-existence of the SCM subcarrier beating-induced cross-talk effect and the transmission loss effect contributes to the occurrence of optimum ω_{RF2} values for the RS modems. In comparison with RS II, the reduction in the optimum

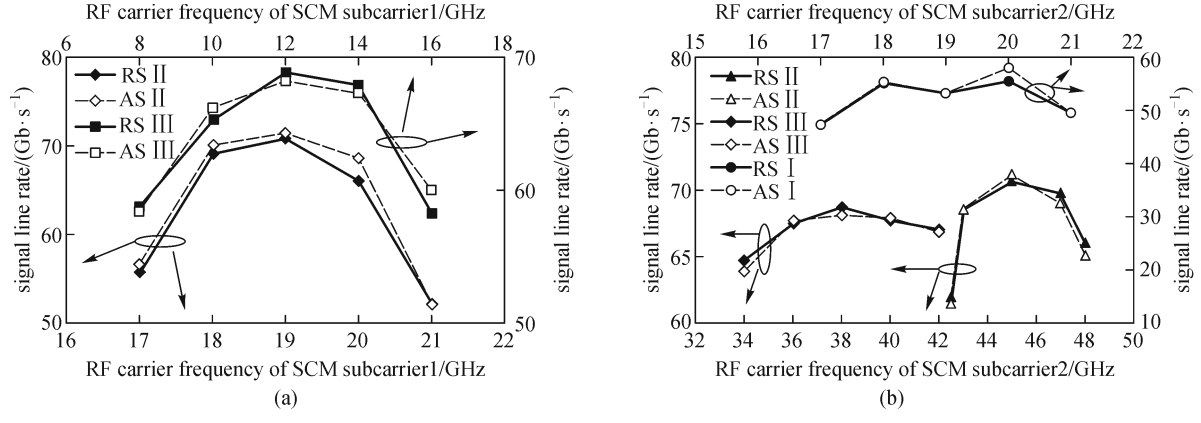

Fig. 4 Optimum SCM subcarrier frequencies for different modem designs. RS: reconfigurable modem; AS: conventional AMOOFDM-SCM scheme. (a) Transmission performance as function of ω_{RF1} for RS (AS) scheme II and III; (b) transmission performance as function of ω_{RF2} for RS (AS) scheme I, II and III

ω_{RF2} value for RS III is a direct result of the use of SSB modulation in RS III. Furthermore, it is also very interesting to note from Fig. 4 that the optimum ω_{RF2} value for RS I is very similar to the optimum ω_{RF1} value for RS II. This confirms the physical origin of the optimum RF frequencies.

In addition, numerical simulations also show that, for RS II and III the optimum ω_{RF1} value is independent of transmission distance, and that an extension of the transmission distance from 40 to 80 km reduces the optimum ω_{RF2} by approximately 1, 4 and 2 GHz for RS I, II and III, respectively. Such behaviours can be explained easily by considering the physical mechanisms discussed above.

Figure 5 shows the maximum achievable transmission performances of RS I, II and III, by taking into account the identified optimum RF frequencies. For performance comparisons and examination of the validity of the proposed modems, achievable transmission performances of AMOOFDM-SCM schemes I, II and III as well as conventional AMOOFDM modems are also plotted in the same figure. It is shown that, over the entire transmission range of up to 100 km, the transmission capacity versus reach performances achieved by the proposed RS modems are almost identical to those supported by the corresponding AMOOFDM-SCM schemes. It should be pointed out, in particular, that such transmission capacities are achieved using the simplified modem designs. This verifies the validity and effectiveness of the proposed RS modems. In comparison with the conventional AMOOFDM modems, the RS modem designs can not only improve the signal transmission capacity versus reach performance by a factor of at least 1.5 for transmission distances of up to 60 km, but also retain excellent performance robustness to variations of the transmission link characteristics.

For short transmission distances of, say less than 20 km, almost no performance difference among the three RS modem designs is observed. This is because the cross-talk effect is much less pronounced owing to short transmission distances [6,7]. Whilst for SMF link lengths in a range from 20 to 40 km, the signal transmission capacities achieved by RS II and III are very similar, which are, however, much higher than those supported by RS I, as shown in Fig. 5. This is due to the use of spectral gaps in RS II and III, which distinguishes the first SCM subcarrier from the unwanted beating products occurring in the vicinity of the optical carrier. Over a transmission distance region of 40–80 km, RS III offers the highest transmission performance due to the SSB SCM subcarrier-induced significant reduction in the cross-talk effect between different SCM subcarriers. Over such a transmission region, the observed rapid performance degradation of RS II originates mainly from an increase in transmission loss due to the employment of a large ω_{RF2} in RS II. The IMDD link frequency response becomes narrow for transmission distances of longer than 80 km, leading to considerable reductions in signal transmission capacity for RS II and III, as their signal bandwidths are much wider than those corresponding to RS I. It is also worth addressing that the proposed RS modems can support transmission capacities of higher than 100 Gb/s by increasing slightly the sampling rates of ADCs/DACs. The sampling rates adopted in the RS modems can, however, be much lower than those predicted in Ref. [4].

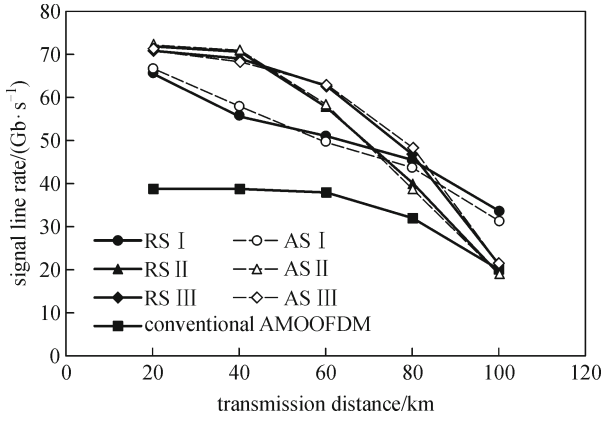

Fig. 5 Signal transmission capacity versus reach performance of different modem designs. RS: reconfigurable modem; AS: AMOOFDM-SCM scheme

5 Conclusions

Three novel RS modems have been proposed, each of which, has a number of salient advantages including a significantly simplified modem configuration due to the involvement of a single IFFT/FFT operation, input/output reconfigurability, dynamic bandwidth allocation capability, cost reduction and system flexibility and performance robustness to variations in transmission link conditions. In addition, the proposed RS modems also offer broadcasting and performance monitoring functionalities. Investigations have shown that RS I, II and III modems are capable of supporting higher than 60 Gb/s signal transmission over 20, 40 and 60 km SMFs respectively in IMDD SMF transmission links without optical amplification and chromatic dispersion compensation.

Acknowledgements This work was partly supported by the European Community's Seventh Framework Programme (FP7/2007-2013) within the project ICT ALPHA under grant agreement number 212352. The work of Zheng and Wei was supported by the School of Electronic Engineering and the Bangor University.

References

1. Tang J M, Shore K A. 30 Gb/s signal transmission over 40-km directly modulated DFB-laser-based single-mode-fiber links

without optical amplification and dispersion compensation. Journal of Lightwave Technology, 2006, 24(6): 2318–2327

2. Shieh W, Bao H, Tang Y. Coherent optical OFDM: theory and design. Optics Express, 2008, 16(2): 841–859
3. Schmidt B J C, Lowery A J, Armstrong J. Experimental demonstrations of electronic dispersion compensation for long-haul transmission using direct detection optical OFDM. Journal of Lightwave Technology, 2008, 26(1): 196–203
4. Jin X Q, Tang J M, Spencer P S, Shore K A. Optimization of adaptively modulated optical OFDM modems for multimode fiber-based local area networks. Journal of Optical Networking, 2008, 7 (3): 198–214
5. Hui R, Zhu B, Huang R, Allen C, Demarest K, Richards D. 10 Gb/s SCM fiber system using optical SSB modulation. IEEE Photonics Technology Letters, 2001, 13(8): 896–898
6. Zheng X, Tang J M, Spencer P S. Transmission performance of adaptively modulated optical OFDM modems using subcarrier modulation over worst-case multimode fibre links. IEEE Communications Letters, 2008, 12(10): 788–790
7. Zheng X, Wei J L, Tang J M. Transmission performance of adaptively modulated optical OFDM modems using subcarrier modulation over SMF IMDD links for access and metropolitan area networks. Optics Express, 2008, 16(25): 20427–20440
8. Giddings R P, Jin X Q, Hugues-Salas E, Giacoumidis E, Wei J L, Tang J M. Experimental demonstration of a record high 11.25 Gb/s real-time optical OFDM transceiver supporting 25 km SMF end-to-end transmission in simple IMDD systems. Optics Express, 2010, 18(6): 5541–5555
9. Jansen S L, Morita I, Schenk T C W, Takeda N, Tanaka H. Coherent optical 25.8 Gb/s OFDM transmission over 4160-km SSMF. Journal of Lightwave Technology, 2008, 26(1): 6–15
10. Carlson A B, Crilly P B, Rutledge J C. Communication Systems: An Introduction to Signals and Noise in Electrical Communication. 4th ed. New York: McGraw-Hill, Higher Education, 2002
11. Wei J L, Hamie A, Giddings R P, Tang J M. Semiconductor optical amplifier-enabled intensity modulation of adaptively modulated optical OFDM signals in SMF-based IMDD systems. Journal of Lightwave Technology, 2009, 27(16): 3678–3688
12. Peng W R, Zhang B, Wu X X, Feng K M, Willner A E, Chi S. Compensation for I/Q imbalances and bias deviation of the Mach-Zehnder modulators in direct-detected optical OFDM systems. IEEE Photonics Technology Letters, 2009, 21(2): 103–105
13. Wei J L, Yang X L, Giddings R P, Tang J M. Colourless adaptively modulated optical OFDM transmitters using SOA as intensity modulators. Optics Express, 2009, 17(11): 9012–9027
14. Choi S I, Huh J D. Dynamic bandwidth allocation algorithm for multimedia services over Ethernet PONs. ETRI Journal, 2002, 24 (6): 465–468
15. Lee J H, Choi K M, Moon J H, Lee C H. Seamless upgrades from a TDM-PON with a video overlay to a WDM-PON. Journal of Lightwave Technology, 2009, 27(15): 3116–3123
16. Tang J M, Lane P M, Shore K A. High-speed transmission of adaptively modulated optical OFDM signals over multimode fibres using directly modulated DFBs. Journal of Lightwave Technology, 2006, 24(1): 429–441
17. Giacoumidis E, Wei J L, Jin X Q, Tang J M. Improved transmission performance of adaptively modulated optical OFDM signals over directly modulated DFB laser-based IMDD links using adaptive cyclic prefix. Optics Express, 2008, 16(13): 9480–9494
18. Tang J M, Shore K A. Maximizing the transmission performance of adaptively modulated optical OFDM signals in multimode-fiber links by optimizing analog-to-digital converters. Journal of Lightwave Technology, 2007, 25(3): 787–798